Multi-step phase transitions and gravitational waves in the inert doublet model

Nico Benincasa, Kristjan Kannike, Luca Marzola and Luigi Delle Rose

arXiv:2205.06669

NICPB, Laboratory of High Energy and Computational Physics, Tallinn

Institute of Physics, University of Tartu

XX Frascati Summer School "Bruno Touschek":
7th Young Researchers' Workshop

July 11, 2022

Outline of the talk

Introduction

Dark matter :

- solution for some problems in astrophysics (galaxy rotation curves, galaxy-cluster collision,...)
- from Planck data, it accounts for 26.8% of the energy content of the Universe...
- ... but one is still ignorant about its nature
- Higgs boson discovery (2012) as an elementary scalar particle
  $\rightarrow$ why not dark matter as well ?

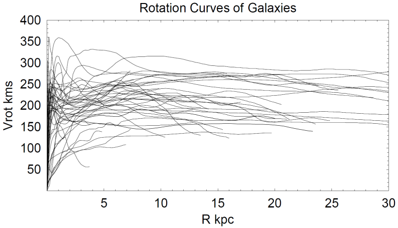

Sofue, arXiv :astro-ph/9906224

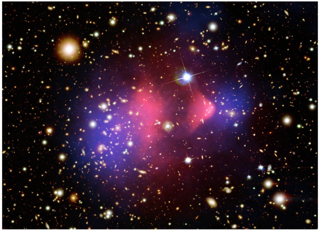

NASA

The whole picture

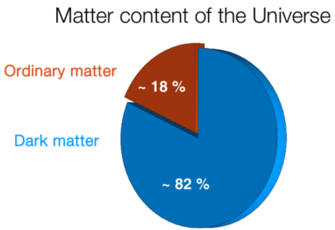

https ://news-g.org/dark-matter/

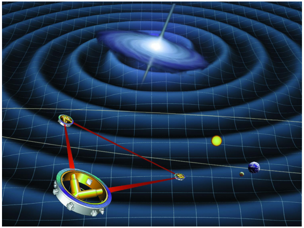

NASA

dark matter → cosmic phase transition → gravitational waves detection

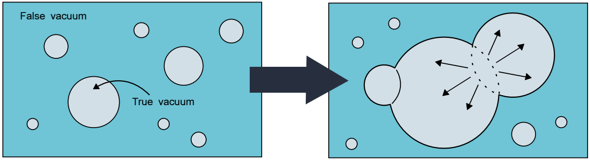

Weir, PoS(CHARGED2018)027

First- and second-order phase transition

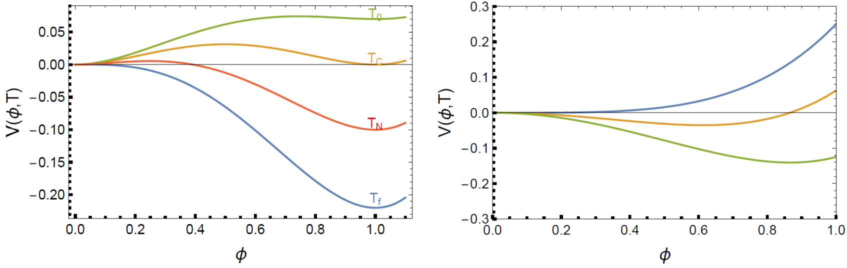

Mazumdar, White, arXiv :1811.01948

- 1st-order phase transitions are abrupt (existence of a barrier) : the order parameter (vev) changes *discontinuously* from zero to a non-zero value
- 2nd-order phase transitions/crossovers are smooth (no barrier) : the order parameter (vev) changes *continuously* from zero to a non-zero value

Thermal phase transition

At high temperature, the false vacuum generally decays through thermal tunneling :

A. D. Linde, Fate of the False Vacuum at Finite Temperature : Theory and Applications, Phys. Lett. B100 (1981) 37.

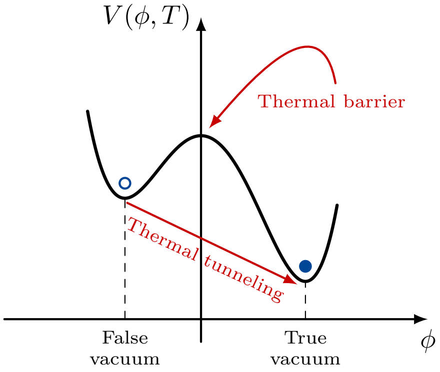

Phase transition

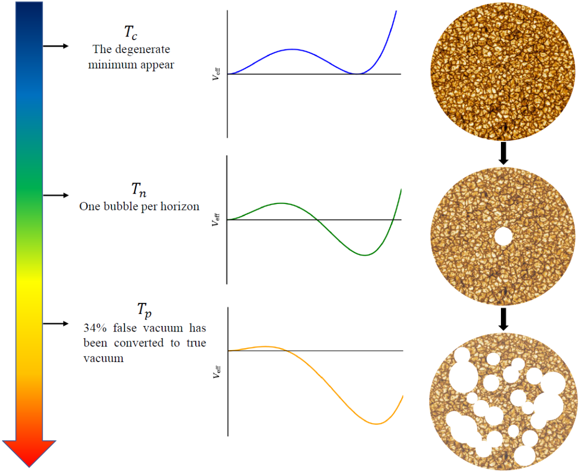

Wang, Huang, Zhang, arXiv :2003.08892

Gravitational waves

- one isolated bubble cannot lead to the production of GWs
- collision between bubbles is the key ingredient to generate a stochastic GW background
- GWs propagate freely $\Rightarrow$ useful tool to probe the early Universe
- processes taking place at this stage of the Universe occur long before the CMB
  $\rightarrow$ GW is the only possible channel

Motivations

- simple SM extension giving rise to 1^{st}-order phase transitions
- gravitational-wave background signals from 1^{st}-order phase transitions could be probed by space-based gravitational-wave detectors such as LISA, BBO or DECIGO
  $\rightarrow$ new way to detect dark matter
- computation of gravitational-wave signal for the whole allowed parameter space not found in the literature
- update : we scan the parameter space considering the most recent phenomenological constraints
- possibility of multi-step phase transitions $\rightarrow$ potentially multiple-peak gravitational-wave signal (specific signature)

Inert doublet model

$\mathbb{Z}_2$-symmetric tree-level potential :

$$V = -m_1^2|H_1|^2 - m_2^2|H_2|^2 + \lambda_1|H_1|^4 + \lambda_2|H_2|^4 + \lambda_3|H_1|^2|H_2|^2 + \lambda_4|H_1^\dagger H_2|^2 + \frac{\lambda_5}{2}\left[(H_1^\dagger H_2)^2 + \mathrm{h.c.}\right],$$

with H_1 and H_2, the Standard-Model Higgs doublet and an inert Higgs doublet respectively. They transform under $\mathbb{Z}_2$ as the following :

$$H_1 \to H_1$$
$$H_2 \to e^{\frac{i2\pi}{2}} H_2 = -H_2.$$

$\mathbb{Z}_2$ symmetry implies that particles can only **appear or disappear in pairs**, so cannot decay.
For instance $\mathbb{Z}_2$ symmetry prevents H_2 from interacting with matter. No Yukawa couplings $\bar{\psi} H_2 \psi$ implies no decay of H_2 into fermions $\to$ stable.

Inert doublet model

H_1 and H_2 are parametrized as

$$H_1 = \begin{pmatrix} G^+ \\ \frac{v+h+iG^0}{\sqrt{2}} \end{pmatrix}, \qquad H_2 = \begin{pmatrix} H^+ \\ \frac{H+iA}{\sqrt{2}} \end{pmatrix},$$

with $v \simeq 246$ GeV, the vev of H_1 at $T = 0$.

Our DM candidate must be neutral $\rightarrow$ it can be either H or A.

In the EW vacuum V is invariant under $H \leftrightarrow A$ except for the term $\sim \lambda_5(H^2 - A^2)$.
$\Rightarrow$ without loss of generality, we choose H as the lightest component of H_2.

All the subsequent results can be kept if A is DM, provided the change $H \leftrightarrow A, \lambda_5 \leftrightarrow -\lambda_5$.

Physical parameters

We replace the parameters $m_1^2, m_2^2, \lambda_1, \lambda_3, \lambda_4$ and λ_5 appearing in V with physical parameters $m_h, m_H, m_A, m_{H^\pm}, v$ and λ_{345}.

Two of them are fixed to the known values :
$v \simeq 246$ GeV and $m_h \simeq 125$ GeV .
$\rightarrow$ the number of independent parameters is reduced by two.

The remaining independent parameters and λ_2 are then further constrained theoretically and by collider searches as well as cosmological observations.

One-loop thermal effective potential

For the treatment of the phase transitions, we suppose that excursions in the field space occur only on the (h, H) plane : we can put all the other fields to zero.

$\Rightarrow$ the tree-level potential becomes

$$V_0(h, H) = -\frac{m_1^2}{2}h^2 + \frac{\lambda_1}{4}h^4 - \frac{m_2^2}{2}H^2 + \frac{\lambda_2}{4}H^4 + \frac{\lambda_{345}}{4}h^2H^2,$$

with $\lambda_{345} \equiv \lambda_3 + \lambda_4 + \lambda_5$.

To V_0 we add quantum corrections V_{CW} and V_{CT} and thermal corrections $V_{1\mathrm{L}}^T$. The resulting full effective thermal potential then reads

$$V_{\mathrm{eff}}(h, H, T) = V_0 + V_{\mathrm{CW}} + V_{\mathrm{CT}} + V_{1\mathrm{L}}^T.$$

Multi-step phase transition :

- one-step phase transition : $O \to h$
- two-step phase transition : $O \to H \to h$ and $O \to Hh \to h$
- three-step phase transition : $O \to H \to Hh \to h$

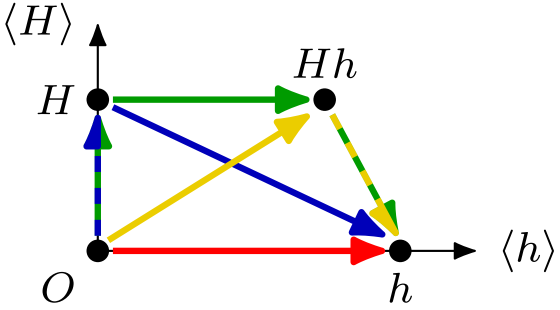

Input parameters for PTs with at least one FOPT step

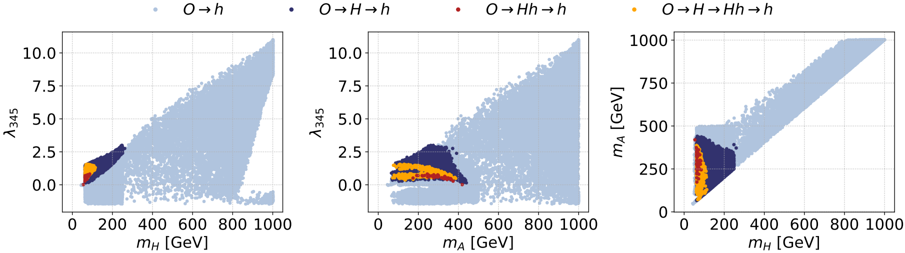

Relic abundance satisfies Planck constraint only for $O \to h$.

Multi-step PT lead to under-abundance only.

Points yielding overabundant DM have been removed.

Spin-independent direct-detection cross section

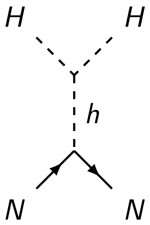

scattering process for direct detection

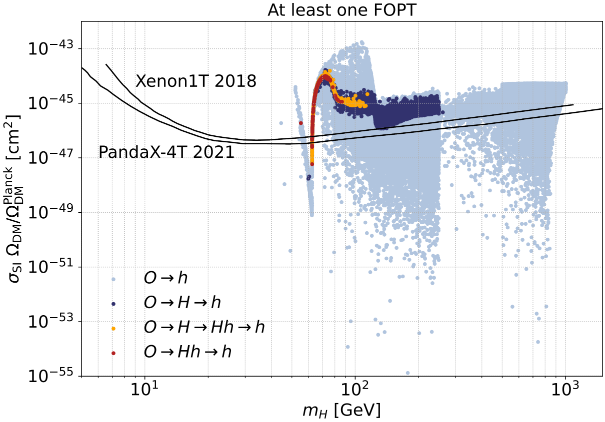

Points yielding overabundant DM have been removed.

GW signal

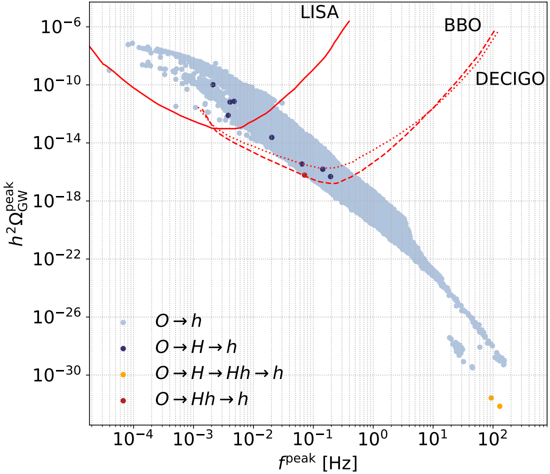

Points yielding overabundant DM and excluded by Xenon1T have been removed.

GW signal and relic density for $O \to h$

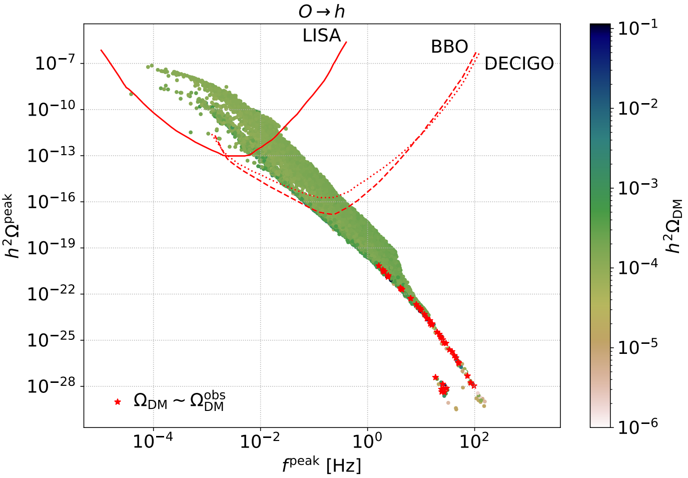

Points yielding overabundant DM and excluded by Xenon1T have been removed.

Double peak ?

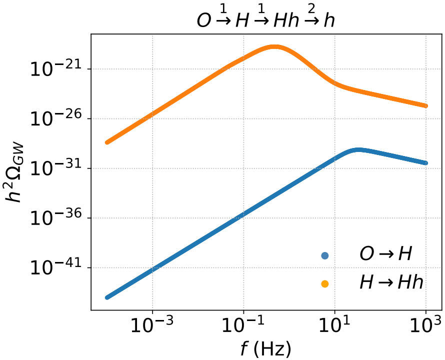

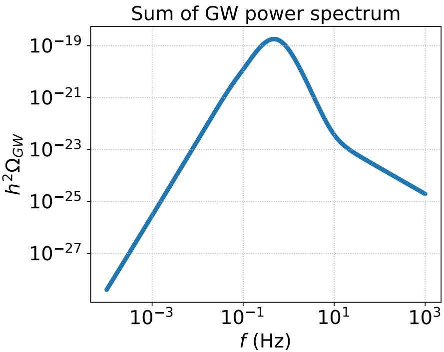

Benchmark point : $m_H = 70$ GeV, $m_A = 400$ GeV, $m_{H^+} = 235$ GeV, $\lambda_2 = 3$ and $\lambda_{345} = 0.6$.

Conclusion

- Although most PTs have a single step ($O \to h$), two-step ($O \to H \to h$ and $O \to hH \to h$) and three-step ($O \to H \to hH \to h$) PTs are possible
- SI-DD constraint allows multi-step PT only around the Higgs-resonance region ($m_H \sim m_h/2$) and $O \to H \to h$ is allowed by Xenon1T for $m_H \in [120, 160]$ GeV
- strongest GW signal from $O \to h$
- LISA, BBO and DECIGO may mainly probe one-step PT
- DM mostly under-abundant and right abundance only found for one-step PT
- no double-peak signal

The End!

Thank you
for your attention!

Any
questions ?

Backup slides

Phase transition parameters

Some definitions :

Grojean, Servant, arXiv :0607107 and Caprini, et al., arXiv :1512.06239

- bubble nucleation rate (or decay rate of the false vacuum) Γ per unit time per unit volume

$$\Gamma/V \sim e^{-S_E(t)}$$

  with S_E the Euclidean action
- inverse time duration of the phase transition

$$\beta \equiv -\frac{dS_E}{dt}\bigg|_{t=t_*}$$

  with t_* the time when GWs are produced

Using the adiabatic time-temperature relation $dT/dt = -H(T)T$, we obtain

$$\frac{\beta}{H_*} = T_* \frac{dS_E}{dT}\bigg|_{T=T_*}$$

with H the Hubble parameter.

Phase transition parameters

Some definitions :

Espinosa, Konstandin, No, Servant, arXiv :1004.4187

- phase transition strength

$$\alpha = \frac{\Delta V_{\text{eff}} - \frac{T}{4}\Delta\frac{\partial V_{\text{eff}}}{\partial T}}{\rho^*_{\text{rad}}}\bigg|_{T=T_*},$$

with $\Delta f \equiv f\big|_{\text{false vacuum}} - f\big|_{\text{true vacuum}}$ and the radiation energy density of the thermal bath

$$\rho^*_{\text{rad}} = g_* \pi^2 T_*^4/30$$

where g_* is the number of relativistic degrees of freedom in the plasma at T_*, the temperature at which GWs are produced

Phase transition parameters

- T_c : critical temperature
- T_n : nucleation temperature
- T_p : percolation temperature

Fast phase transitions ($t \ll H^{-1}$) $\Rightarrow T_n \simeq T_p$.
Kobakhidze, Lagger, Manning, Yue, arXiv :1703.06552

At T_n, one bubble has nucleated per Hubble time per Hubble volume :

$$\Gamma H^{-4} \sim O(1).$$

Gravitational waves

- one isolated bubble cannot lead to the production of GWs
- collision between bubbles is the key ingredient to generate a stochastic GW background
- GWs propagate freely $\Rightarrow$ useful tool to probe the early Universe
- processes taking place at this stage of the Universe occur long before the CMB
  $\rightarrow$ GW is the only possible channel
- The power spectrum Ω_{GW} of GWs from 1^{st}-order phase transitions consists of three different contributions that should, at least approximately, linearly combine :
  Caprini, et al., arXiv :1512.06239

$$\Omega_{\text{GW}} \simeq \Omega_{\phi} + \Omega_{\text{sw}} + \Omega_{\text{turb}}$$

Scalar field ϕ

- part of the released vacuum energy is transmitted to the bubble
- envelope approximation : this part is essentially contained in a thin shell near the bubble wall

  Kosowsky, Turner, arXiv :9211004
- short-lasting process : when bubbles collide, the energy contained in the shells quickly disperse
- conversion of vacuum energy into the scalar field gradient energy is not so efficient
- brief process + inefficient conversion $\rightarrow \Omega_\phi$ is negligible in non-runaway scenarios

Sound waves

- based on sound shell model
  Hindmarsh, arXiv :1608.04735
- detonation $\rightarrow$ rarefaction wave behind the bubble wall
- deflagration $\rightarrow$ compression wave beyond the bubble wall
- overlapping of sound wave shells $\rightarrow$ GW production
- long-lasting process : sound waves remain a long time after bubbles have collided

MHD turbulence

- turbulence after bubble collision
- at most $5 - 10\%$ of the bulk motion is converted into turbulence (the other part into sound waves)
  Hindmarsh, arXiv :1504.03291
- long-lasting process : acts as a source of GWs for several Hubble times

Gravitational-wave production : summary

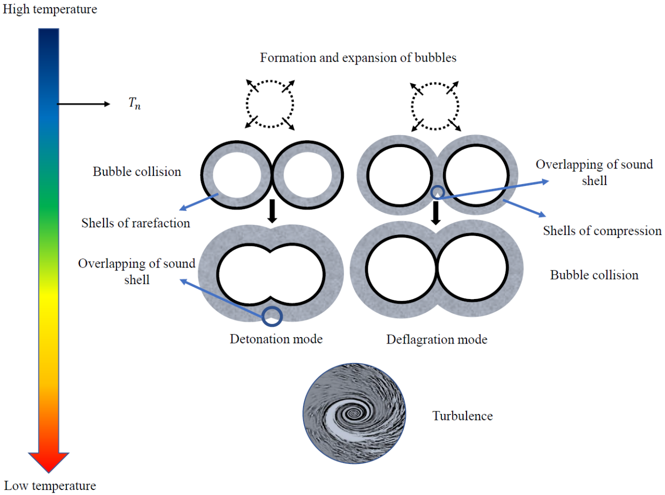

Wang, Huang, Zhang arXiv :2003.08892

Possible scenarios

Depending on the velocity of the bubble wall, three scenarios are possible :

Caprini, et al., arXiv :1512.06239

- Non-runaway bubbles : terminal velocity for the bubble wall due to friction from the plasma $\rightarrow \Omega_{\mathrm{GW}} \simeq \Omega_{\mathrm{sw}} + \Omega_{\mathrm{turb}}$
- Runaway bubbles in a plasma : bubble wall velocity tends to the speed of light $\rightarrow \Omega_{\mathrm{GW}} \simeq \Omega_{\phi} + \Omega_{\mathrm{sw}} + \Omega_{\mathrm{turb}}$
- Runaway bubbles in vacuum : bubble wall velocity tends to the speed of light $\rightarrow \Omega_{\mathrm{GW}} \simeq \Omega_{\phi}$

Parametrization

The requirement that the tree-level potential be minimized at the EW vacuum and m_h^2, m_H^2, m_A^2 and $m_{H^\pm}^2$ ($m_{G^0} = m_{G^\pm} = 0$ in the EW vacuum) to be the eigenvalues of the tree-level mass matrix, leads to the following parametrization :

$$m_1^2 = \frac{m_h^2}{2}, \quad m_2^2 = -m_H^2 + \lambda_{345}\frac{v^2}{2}, \quad \lambda_1 = \frac{m_h^2}{2v^2},$$

$$\lambda_3 = \lambda_{345} + 2\frac{m_{H^\pm}^2 - m_H^2}{v^2}, \quad \lambda_4 = \frac{m_H^2 + m_A^2 - 2m_{H^\pm}^2}{v^2}$$

$$\text{and} \quad \lambda_5 = \frac{m_H^2 - m_A^2}{v^2},$$

with $\lambda_{345} = \lambda_3 + \lambda_4 + \lambda_5$.
H being the lightest component of H_2 implies $\lambda_5 < 0$ and $\lambda_4 + \lambda_5 = \lambda_4 - |\lambda_5| < 0$.

Charged vacuum ?

if vev for $H^{\pm}$, the charged component of H_2 :

- would break $U(1)_{\mathrm{EM}}$ (because of $H^{\pm}\gamma\gamma$ coupling)
  $\rightarrow$ electric-charge non-conservation and massive photon
- H is the lightest component $\rightarrow \lambda_4 - |\lambda_5| < 0$...
- ... in contradiction with $\lambda_4 + \lambda_5 > 0$, needed for $H^{\pm}$ to develop a vev.

Ginzburg, Kanishev, Krawczyk, Sokolowska, arXiv :1009.4593

Theoretical constraints

- stability of the potential : bounded-from-below potential
- H is the lightest component of H_2 : $\lambda_4 - |\lambda_5| < 0$
- global minimum at $T = 0$: $(h, H) = (v, 0)$
- perturbative unitarity : scattering matrix such that $SS^\dagger = \mathbb{1}$

$$\Rightarrow |\text{Re } a_0^i| \leq \frac{1}{2} \quad \forall i$$

with a_0^i the eigenvalues of a_0, the 0^{th} partial wave amplitude

Experimental constraints

LEP :

- LEP I : precise measurements of Z and W decay width forbids decay of Z and W into dark-sector particles :

  Cao, Ma, Rajasekaran, arXiv :0708.2939

$$m_H + m_{H^\pm} > m_W, \quad m_A + m_{H^\pm} > m_W,$$
$$m_H + m_A > m_Z, \quad 2m_{H^\pm} > m_Z$$

- LEP II : $m_H < 80$ GeV $\wedge$ $m_A < 100$ GeV $\wedge$ $m_A - m_H > 8$ GeV is excluded, while $m_{H^\pm} > 70$ GeV is allowed

  Lundström, Gustafsson, Edsjö, arXiv : 0810.3924

  Pierce, Thaler, arXiv : hep-ph/0703056

- EWPT : 0 GeV $< m_{H^\pm} - m_A <$ 100 GeV

  Belyaev, Cacciapaglia, Ivanov, Rojas-Abatte, Thomas, arXiv : 1612.00511

Experimental constraints

- Higgs invisible branching ratio :
  If $2m_H \leq m_h \simeq 125$ GeV, $h \to HH$ may occur $\Rightarrow$ invisible Higgs decay

$$\mathrm{Br}(h \to HH) = \frac{\Gamma(h \to HH)}{\Gamma_h^{\mathrm{SM}} + \Gamma(h \to HH)} < 0.23 - 0.36,$$

  CMS Collaboration, arXiv : 1610.09218

  ATLAS Collaboration, arXiv : 1909.02845

  with Γ_h^{SM} the Higgs total decay width in the Standard Model
- dark-matter relic density : $\Omega_{\mathrm{DM}} h^2 = 0.120 \pm 0.001$

  Planck Collaboration, arXiv :1807.06209

  where h is the dimensionless Hubble parameter, $H = 100\,h\,\mathrm{km/s/Mpc}$.

Relic density

$\sigma \sim$

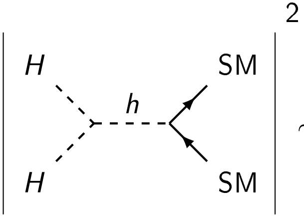

$\sim \lambda_{345}^2$

$$\Omega_{\mathrm{DM}} h^2 \sim \frac{1}{\langle \sigma v \rangle} \sim \frac{1}{\lambda_{345}^2} \to \text{ constraint on } \lambda_{345}.$$

Relic density

$$\Omega_{\mathrm{DM}} h^2 \sim \frac{1}{\langle \sigma v \rangle} \sim \frac{1}{\lambda_{345}^2} \rightarrow \text{ constraint on } \lambda_{345}.$$

Abundance of H can for instance satisfy $\Omega_{\mathrm{DM}} h^2 = 0.120 \pm 0.001$

Diaz, Koch, Urrutia-Quiroga, arXiv :1511.04429

- for $m_H \in [3, 50]$ GeV (ruled out by $R_{\gamma\gamma} \rightarrow 0$, due to $h \rightarrow HH$, and by SI DD cross-section experiment)
- in the Higgs funnel region ($m_H \sim m_h/2$)
- for $m_H > 500$ GeV

or

Blinov, Kozaczuk, Morrissey, de la Puente, arXiv :1510.08069

- for compressed mass spectrum ($m_A - m_H \ll 1$ GeV and $m_{H^\pm} - m_{A,H} \gtrsim 1$ GeV)
- under-abundant for $m_Z/2 \leq m_H \leq 500$ GeV

Experimental constraints

Constraint on spin-independent direct-detection cross section :

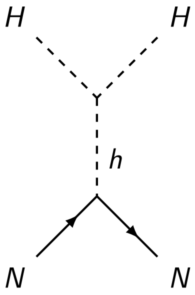

scattering process for direct detection

Experimental constraints

Constraint on spin-independent direct-detection cross section :

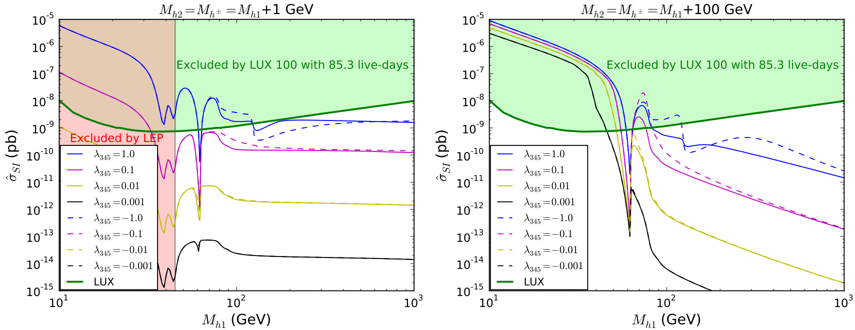

Belyaev, Cacciapaglia, Ivanov, Rojas-Abatte, Thomas, arXiv :1612.00511

where $\hat{\sigma}_{\mathrm{SI}} = R_\Omega \times \sigma_{\mathrm{SI}}$, with $R_\Omega \equiv \Omega_{\mathrm{DM}}/\Omega_{\mathrm{DM}}^{\mathrm{Planck}}$ a scaling factor taking into account the case where DM is under-abundant.

One-loop thermal effective potential

We study the phase transitions in the early Universe : large temperature $\Rightarrow$ finite-temperature quantum field theory must be used to take thermal effects into account.
The resulting full effective thermal potential reads

$$V_{\text{eff}} = V_0 + V_{\text{CW}} + V_{\text{CT}} + V_{1\text{L}}^T$$

- V_0 : tree-level potential
- V_{CW} : $T = 0$ Coleman–Weinberg potential
- V_{CT} : counterterms
- $V_{1\text{L}}^T$: one-loop thermal corrections

One-loop thermal effective potential

For the treatment of the phase transitions, we suppose that excursions in the field space occur only on the (h, H) plane : no vev (at any T) for the remaining scalar degrees of freedom.
$\Rightarrow$ the tree-level potential

$$V = -m_1^2|H_1|^2 - m_2^2|H_2|^2 + \lambda_1|H_1|^4 + \lambda_2|H_2|^4 + \lambda_3|H_1|^2|H_2|^2 \\ + \lambda_4|H_1^\dagger H_2|^2 + \frac{\lambda_5}{2}\left[(H_1^\dagger H_2)^2 + \text{h.c.}\right],$$

becomes

$$V_0(h, H) = -\frac{m_1^2}{2}h^2 + \frac{\lambda_1}{4}h^4 - \frac{m_2^2}{2}H^2 + \frac{\lambda_2}{4}H^4 + \frac{\lambda_{345}}{4}h^2 H^2,$$

with $\lambda_{345} = \lambda_3 + \lambda_4 + \lambda_5$.

One-loop thermal effective potential

$$V_{\text{eff}} = V_0 + V_{\text{CW}} + V_{\text{CT}} + V_{1\text{L}}^T$$

In Landau gauge, the second term, V_{CW}, is defined in the $\overline{\text{MS}}$ scheme as

$$V_{\text{CW}}(h, H) = \frac{1}{64\pi^2} \sum_i (-1)^F g_i \, M_i^4(h, H) \left[\ln \frac{M_i^2(h, H)}{\mu_0^2} - C_i \right],$$

where

- g_i : the number of degrees of freedom
- $M_i^2(h, H)$: i^{th} eigenvalue of the field-dependent mass matrix $(M^2)_{ab} \equiv \partial^2 V / \partial\phi_a \partial\phi_b$
- μ_0 : renormalisation scale (we take $\mu_0 = v$)
- $F = 1$ for fermions and $F = 0$ for bosons
- $C_i = 3/2$ for scalars, fermions and longitudinal gauge bosons and $C_i = 1/2$ for transverse gauge bosons

One-loop thermal effective potential

$$V_{\text{eff}} = V_0 + V_{\text{CW}} + V_{\text{CT}} + V_{1\text{L}}^T$$

The third term, V_{CT}, contains the finite parts of the counterterms that are fixed such that the scalar vevs and masses remain at their tree-level values at the $T = 0$ global minimum (v, 0) :

$$V_{\text{CT}}(h, H) = \delta m_h^2 h^2 + \delta m_H^2 H^2 + \delta\lambda_1 h^4 \,,$$

such that the following renormalization conditions are satisfied :

$$\left.\frac{\partial V_{\text{CT}}}{\partial h}\right|_{\text{vev}} = -\left.\frac{\partial V_{\text{CW}}}{\partial h}\right|_{\text{vev}},$$

$$\left.\frac{\partial^2 V_{\text{CT}}}{\partial h^2}\right|_{\text{vev}} = \left.\left(-\frac{\partial^2 V_{\text{CW}}|_{G\equiv 0}}{\partial h^2} + \frac{1}{32\pi^2}\sum_{G=G^0,G^\pm}\left(\frac{\partial m_G^2}{\partial h}\right)^2 \ln\left(\frac{m_{\text{IR}}^2}{\mu^2}\right)\right)\right|_{\text{vev}},$$

$$\left.\frac{\partial^2 V_{\text{CT}}}{\partial H^2}\right|_{\text{vev}} = \left.\left(-\frac{\partial^2 V_{\text{CW}}|_{G\equiv 0}}{\partial H^2} + \frac{1}{32\pi^2}\sum_{G=G^0,G^\pm}\left(\frac{\partial m_G^2}{\partial H}\right)^2 \ln\left(\frac{m_{\text{IR}}^2}{\mu^2}\right)\right)\right|_{\text{vev}}.$$

One-loop thermal effective potential

$$V_{\text{eff}} = V_0 + V_{\text{CW}} + V_{\text{CT}} + V_{1\text{L}}^T.$$

The last term, $V_{1\text{L}}^T$, is defined as

$$V_{1\text{L}}^T(h, H, T) = \frac{T^4}{2\pi^2} \sum_i g_i \, J_{\text{B/F}} \left(\frac{M_i^2(h, H)}{T^2} \right)$$

with

$$J_{\text{B/F}}(y^2) = (-1)^F \int_0^\infty x^2 \log \left[1 \mp e^{-\sqrt{x^2+y^2}} \right]$$

- T : temperature
- g_i : degrees of freedom of the i^{th} particle
- $M_i^2(h, H)$: i^{th} eigenvalue of the field-dependent mass matrix $(M^2)_{ab} \equiv \partial^2 V / \partial\phi_a \partial\phi_b$

High-temperature expansion

In the high-temperature limit ($|y^2| = |M_i^2/T^2| \ll 1$), we can expand the thermal function J as following :

Curtin, Meade, Ramani, arXiv :1612.00466

$$J_B(y^2) \approx -\frac{\pi^4}{45} + \frac{\pi^2}{12}y^2 - \frac{\pi}{6}y^3 - \frac{1}{32}y^4 \log\left(\frac{y^2}{a_b}\right)$$
$$J_F(y^2) \approx -\frac{7\pi^4}{360} + \frac{\pi^2}{24}y^2 + \frac{1}{32}y^4 \log\left(\frac{y^2}{a_f}\right)$$

- $a_b = \pi^2 \exp(3/2 - 2\gamma_E)$
- $a_f = 16\pi^2 \exp(3/2 - 2\gamma_E)$

with $\gamma_E \simeq 0.577$, the Euler–Mascheroni constant.

High-temperature expansion

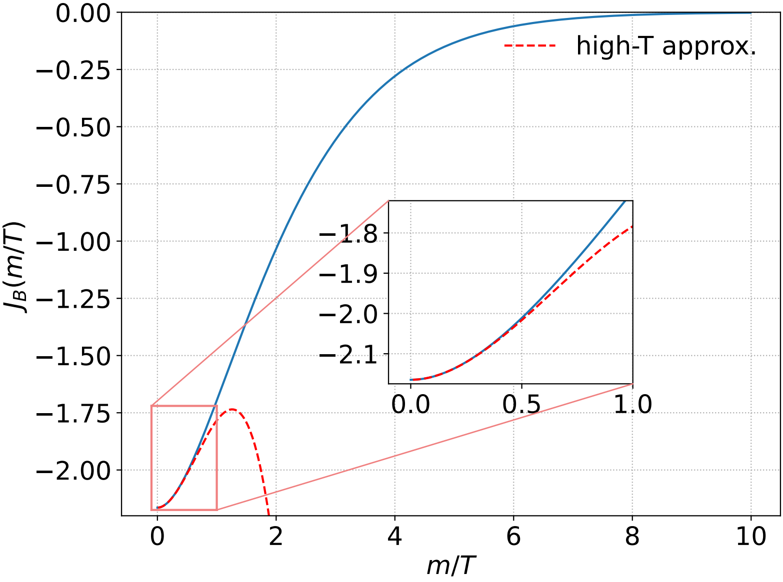

Imaginary contributions

The cubic term in

$$J_B(y^2) \approx -\frac{\pi^4}{45} + \frac{\pi^2}{12} y^2 - \frac{\pi}{6} y^3 - \frac{1}{32} y^4 \log\left(\frac{y^2}{a_b}\right)$$

can be imaginary for $M_i^2 < 0$. Indeed,

$$y^3 = (y^2)^{3/2} = \left(\frac{M_i^2}{T^2}\right)^{3/2}$$

$$\Rightarrow \operatorname{Im} y^3 \neq 0 \quad \text{for} \quad M_i^2 < 0$$

Likewise for the $\ln M_i^2$ term in V_{CW}.

$\Rightarrow$ Thus we always consider the real part of V_{eff} in our calculations.

Thermal resummation

Finally, we use the thermally improved finite-temperature potential, which is obtained by adding to the field-dependent masses in V_{CW} and $V_{1\mathrm{L}}^{T}$ the leading thermal corrections :

$$M_i^2(h,H) \to M_i^2(h,H) + c_i T^2,$$

where the coefficients c_i are given by

$$\begin{aligned} c_h &= \frac{1}{16}(g_1^2 + 3g_2^2) + \frac{1}{4}y_t^2 + \frac{6\lambda_1 + 2\lambda_3 + \lambda_4}{12}\,, \\ c_H &= \frac{1}{16}(g_1^2 + 3g_2^2) + \frac{6\lambda_2 + 2\lambda_3 + \lambda_4}{12} \end{aligned}$$

for the scalars.

Parameter-space scan

Range of parameters :

Belyaev, et al., arXiv :1612.00511

- $m_H \in [10, 1000]$ GeV
- $m_A \in [m_H, 1000 \text{ GeV}]$
- $m_{H^\pm} \in [m_H, 1000 \text{ GeV}]$
- $\lambda_2 \in [0, 4\pi/3]$ (vacuum stability and perturbative unitarity)
- $\lambda_{345} \in [-1.47, 4\pi]$ (vacuum stability and perturbative unitarity)
- we consider the runaway-bubble-in-plasma scenario ($v_w \sim 1$)
- we use micrOMEGAs and CosmoTransitions, respectively, to compute the relic density and the phase-transition parameters

These ranges are further constrained by the remaining theoretical/experimental constraints.

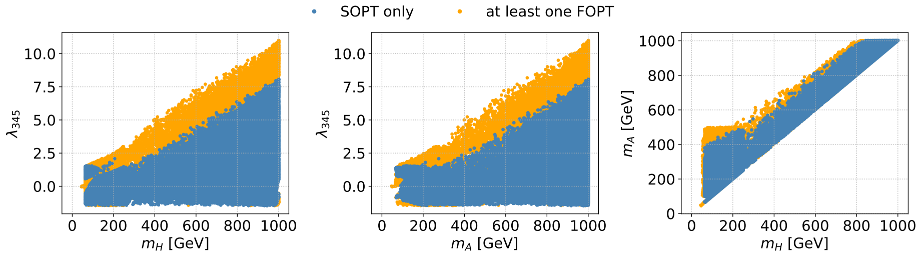

Points yielding overabundant DM have been removed.

Input parameters ($O \to h$)

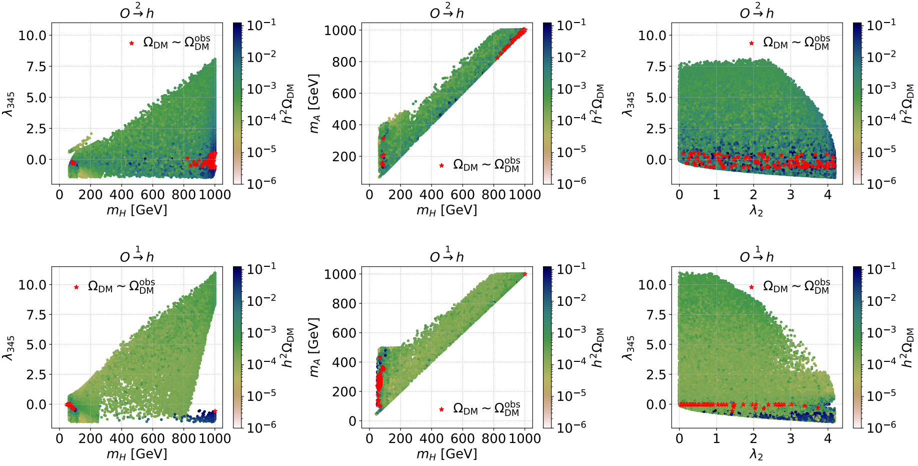

Points yielding overabundant DM have been removed.

Input parameters ($O \to H \to h$)

This phase transition is mostly of the first-order kind :

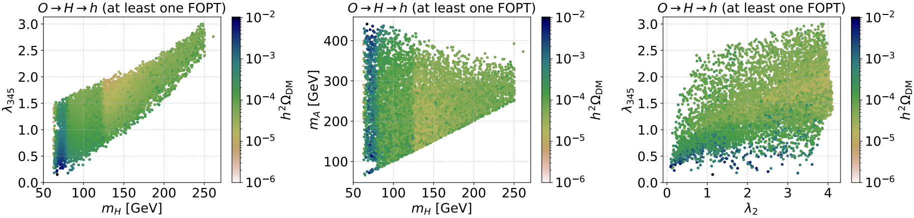

Narrower parameter space for $O \to H \to h$ (at least one FOPT) :

- $m_H \leq 250$ GeV
- $m_{A,H^\pm} \leq 500$ GeV
- $\lambda_{345} \in [0, 3]$
- unchanged for λ_2 : $[0, 4]$
- under-abundant dark matter

Points yielding overabundant DM have been removed.

Input parameters ($O \to Hh \to h$)

This phase transition is mostly of first-order kind :

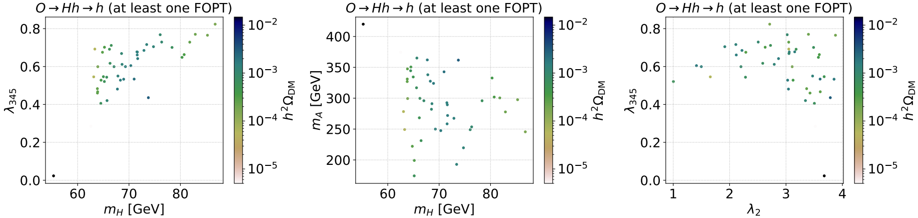

Even narrower parameter space for $O \to Hh \to h$ (at least one FOPT) :

- $m_H \leq 90$ GeV
- $m_{A,H^{\pm}} \leq 450$ GeV
- $\lambda_{345} \in [0, 0.9]$
- $\lambda_2 \in [1, 4]$
- under-abundant dark matter

Points yielding overabundant DM have been removed.

Input parameters ($O \to H \to Hh \to h$)

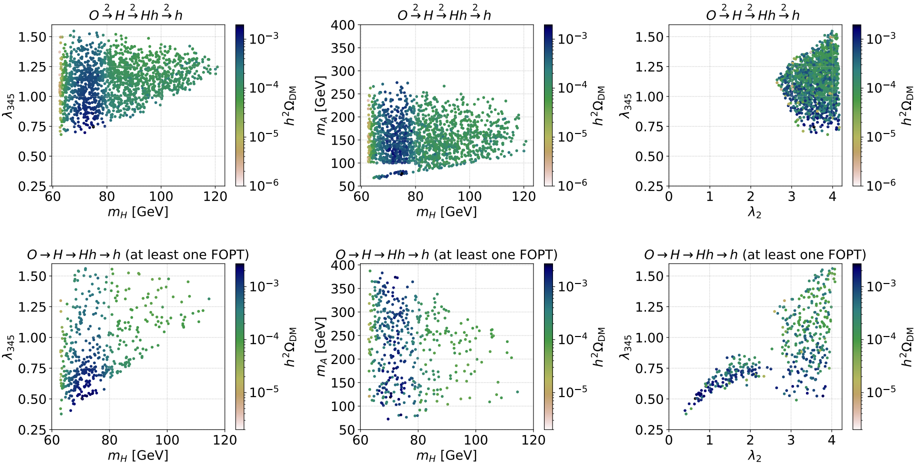

Points yielding overabundant DM have been removed.

Phase-transitions parameters

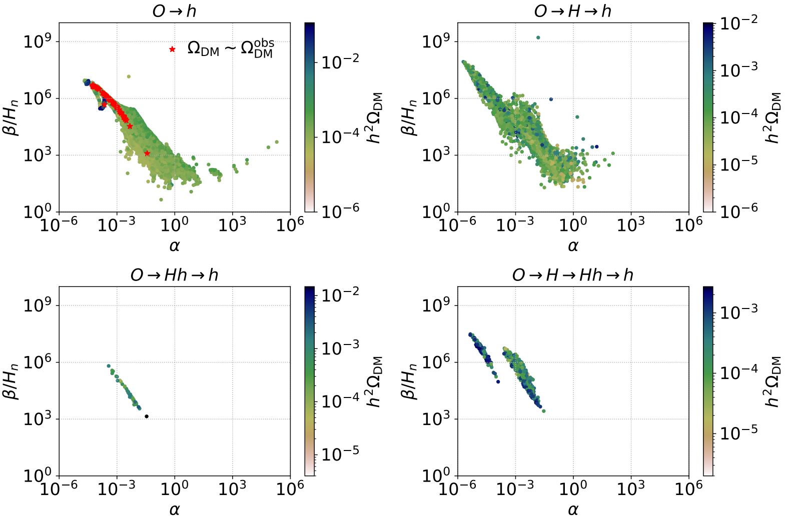

Points yielding overabundant DM have been removed.

T_n vs T_c

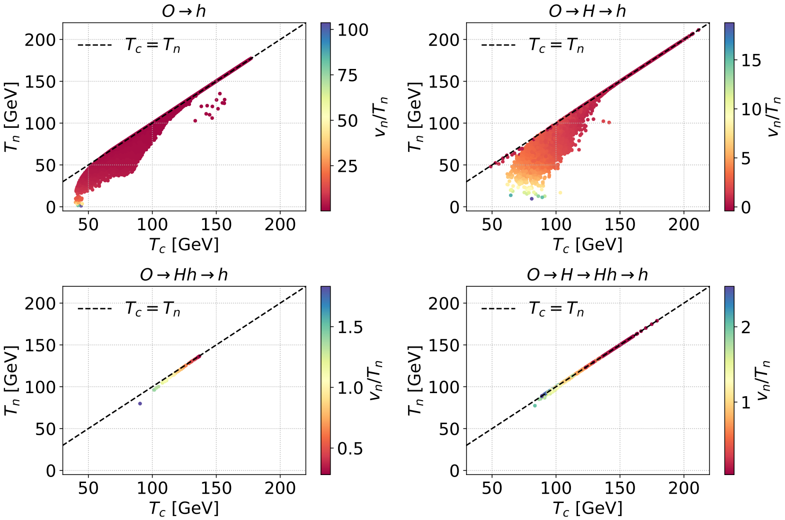

Points yielding overabundant DM have been removed.

Monojet search

Projected limit on λ_{345} from $pp \to HHj$ at 13 TeV :

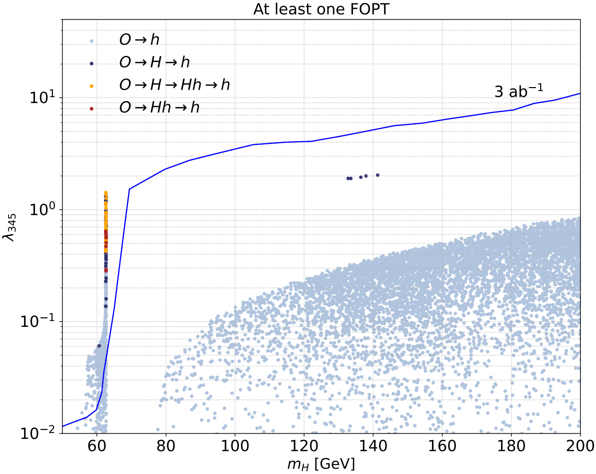

Points yielding overabundant DM and excluded by Xenon1T have been removed.

Feynman diagrams for the projected limit on λ_{345} from $pp \to HHj$ at 13 TeV

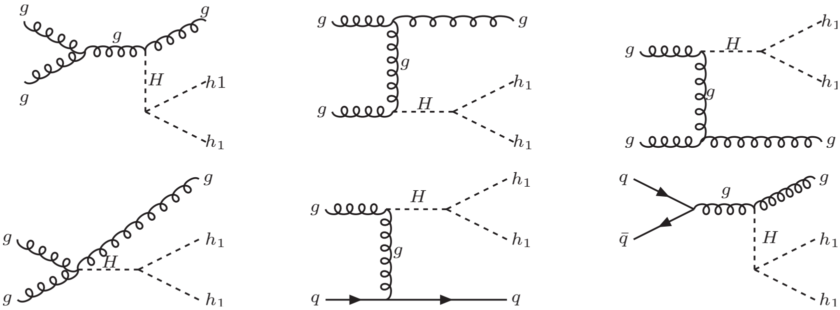

Belyaev, Cacciapaglia, Ivanov, Rojas-Abatte, Thomas, arXiv :1612.00511

Input parameters ($O \rightarrow h$) allowed by Xenon1T and LISA

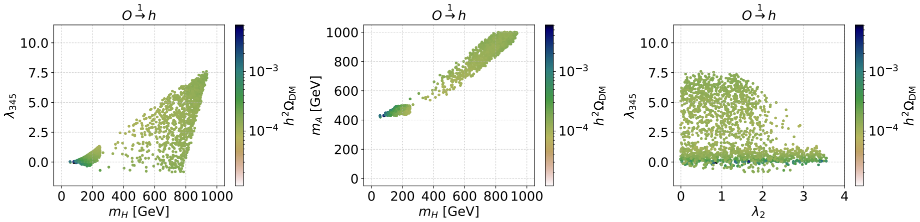

Points yielding overabundant DM and excluded by Xenon1T and LISA have been removed.

Benchmark point

m_H (GeV)	phase transition	T_c (GeV)	α	β/H_n	$\Omega_H/\Omega_{\rm DM}$
	$\mathbf{O} \xrightarrow{2} \mathbf{H} \xrightarrow{1} Hh \xrightarrow{2} h$	158.62	0	0	
10	$O \xrightarrow{2} \mathbf{H} \xrightarrow{1} \mathbf{Hh} \xrightarrow{2} h$	112.59	2.82×10^{-3}	8.00×10^{4}	0.106
	$O \xrightarrow{2} H \xrightarrow{1} \mathbf{Hh} \xrightarrow{2} \mathbf{h}$	17.09	0	0	
$\vdots$	$\vdots$	$\vdots$	$\vdots$	$\vdots$	$\vdots$
	$\mathbf{O} \xrightarrow{2} \mathbf{H} \xrightarrow{1} Hh \xrightarrow{2} h$	148.93	0	0	
40	$O \xrightarrow{2} \mathbf{H} \xrightarrow{1} \mathbf{Hh} \xrightarrow{2} h$	113.02	3.60×10^{-3}	5.01×10^{4}	0.038
	$O \xrightarrow{2} H \xrightarrow{1} \mathbf{Hh} \xrightarrow{2} \mathbf{h}$	73.20	0	0	
	$\mathbf{O} \xrightarrow{1} \mathbf{H} \xrightarrow{1} Hh \xrightarrow{2} h$	142.70	1.06×10^{-6}	2.33×10^{8}	
50	$O \xrightarrow{1} \mathbf{H} \xrightarrow{1} \mathbf{Hh} \xrightarrow{2} h$	113.68	4.03×10^{-3}	4.00×10^{4}	0.014
	$O \xrightarrow{1} H \xrightarrow{1} \mathbf{Hh} \xrightarrow{2} \mathbf{h}$	85.73	0	0	
$\vdots$	$\vdots$	$\vdots$	$\vdots$	$\vdots$	$\vdots$
	$\mathbf{O} \xrightarrow{1} \mathbf{H} \xrightarrow{1} Hh \xrightarrow{2} h$	121.13	1.26×10^{-5}	6.37×10^{6}	
70	$O \xrightarrow{1} \mathbf{H} \xrightarrow{1} \mathbf{Hh} \xrightarrow{2} h$	115.45	5.43×10^{-3}	2.16×10^{4}	0.004
	$O \xrightarrow{1} H \xrightarrow{1} \mathbf{Hh} \xrightarrow{2} \mathbf{h}$	107.36	0	0	
80	$\mathbf{O} \xrightarrow{1} \mathbf{h}$	116.32	6.65×10^{-3}	1.13×10^{4}	0.001
$\vdots$	$\vdots$	$\vdots$	$\vdots$	$\vdots$	$\vdots$
210	$\mathbf{O} \xrightarrow{1} \mathbf{h}$	138.47	3.39×10^{-4}	2.32×10^{3}	0.002
220	$\mathbf{O} \xrightarrow{2} \mathbf{h}$	139.84	0	0	0.002
230	$\mathbf{O} \xrightarrow{2} \mathbf{h}$	141.36	0	0	0.002

BM point : $m_A = 400$ GeV, $m_{H^+} = 235$ GeV, $\lambda_2 = 3$ and $\lambda_{345} = 0.6$, with variation of m_H. The quantity $\Omega_H/\Omega_{\rm DM}$ is the fraction that the inert scalar H contributes to the relic density.

GW signal for a benchmark point

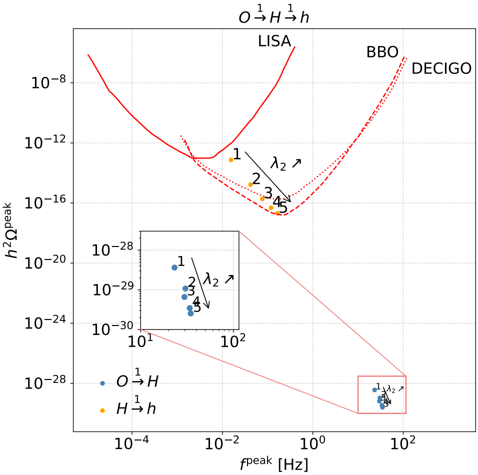

BM point : $m_H = 70$ GeV, $m_A = 400$ GeV, $m_{H^+} = 235$ GeV, $\lambda_{345} = 0.6$ and $\lambda_2 \in [0.7, 1.1]$.

GW signal for a benchmark point

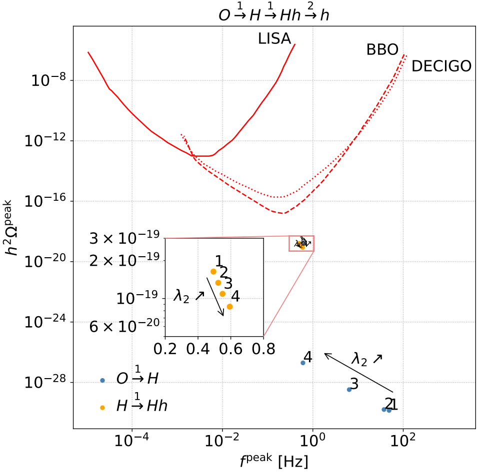

BM point : $m_H = 68$ GeV, $m_A = 398$ GeV, $m_{H^+} = 233$ GeV, $\lambda_{345} = 0.6$ and $\lambda_2 \in [2.9, 3.2]$.

New W mass measurement

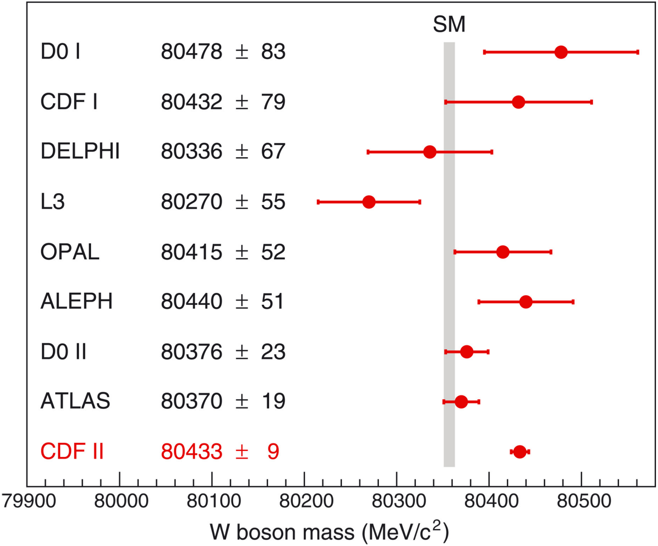

CDF Collaboration

New W mass constraint on input parameters

PDG m_W :

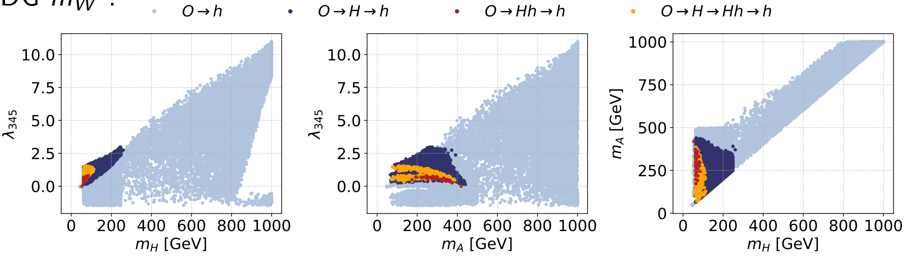

CDF m_W :

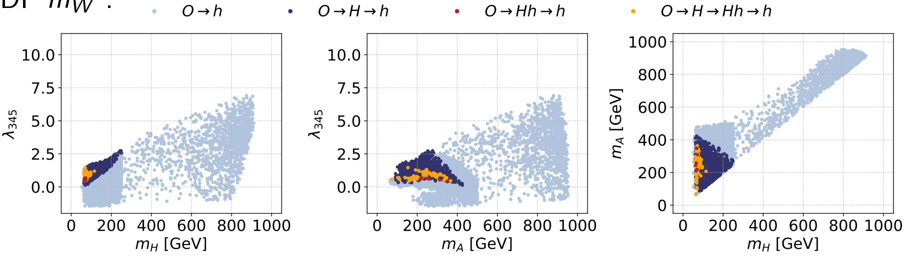

Points yielding overabundant DM have been removed.

New W mass constraint on SI DD and GW signal

- SI DD signal :

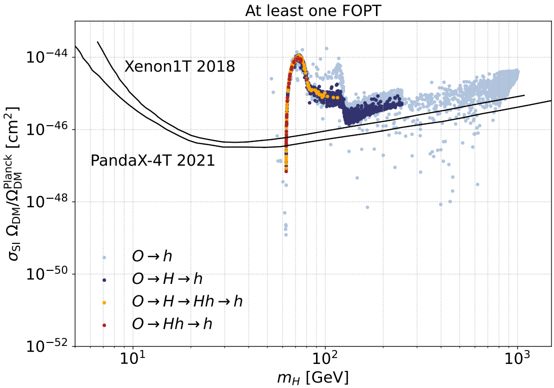

Points yielding overabundant DM

- GW signal basically not impacted